RSC Advances

This article can be cited before page numbers have been issued, to do this please use: H. Shen, G. Zhu, W. B. Yu, H. Wu, H. Ji, H. Shi, Y. zheng and Y. She, *RSC Adv.*, 2015, DOI: 10.1039/C5RA15592D.

ROYAL SOCIETY OF CHEMISTRY

www.rsc.org/advances

View Article Online
DOI: 10.1039/C5RA15592D

RSC Advances

ARTICLE

Surface immobilization of β-cyclodextrin on hybrid silica and its fast-adsorption performance to p-nitrophenol from aqueous phase

Received 00th January 20xx,
Accepted 00th January 20xx

DOI: 10.1039/x0xx00000x

www.rsc.org/

Hai-Min Shen,[a] Gong-Yuan Zhu,[a] Wu-Bin Yu,[a] Hong-Ke Wu,[a] Hong-Bing Ji,[b] Hong-Xin Shi,[a] Yi-Fan Zheng*[a] and Yuan-Bin She*[a]

Renewable β-cyclodextrin (β-CD) was immobilized onto the surface of hybrid silica using ethylenediamine as linking groups to construct adsorbent in water treatment (CD@Si), and the obtained CD@Si was characterized through FT-IR, XPS, EDX, contact angle measurement, TGA, solid-state ^{13}C NMR, SEM, and XRD analyses. The effect of initial pH, contact time on the adsorption performance of CD@Si to p-nitrophenol, and the adsorption kinetics, adsorption isotherms, adsorption thermodynamics, reusability and adsorption mechanism were investigated systematically, which indicate the adsorption of p-nitrophenol onto CD@Si is a very fast process, the adsorption equilibrium can be reached in 15 s with acceptable equilibrium adsorption capacity of 69.6 mg/g in pH = 7.0, much faster than many reported adsorbents based on β-CD. The adsorption of p-nitrophenol onto CD@Si follows the pseudo-second-order model, obeys the Freundlich model, and is a feasible, spontaneous, and exothermic process which is more favorable in lower temperature. And the formation of inclusion complex and hydrogen bond interaction are two origins of p-nitrophenol being adsorbed onto CD@Si. Additionally, CD@Si can be recycled and reused at least five runs with acceptable adsorption capacity, is a very promising adsorbent in the fast adsorption of p-nitrophenol or its analogues from aqueous phase. Additionally, this work also provides a strategy to increase the adsorption rate of adsorbent based on β-CD.

1. Introduction

In modern society, a variety of organic molecules are discharged into the natural environment as the rapid development of industrialization and urbanization. Most of these organic molecules do not exist in the environment naturally and can cause many serious environmental problems such as water pollution for the negative effect of the organic molecules on human health and ecological systems. p-Nitrophenol is an important chemical raw material and intermediate in the production of pharmaceuticals, pesticides, dyes, artificial resins, explosives, and other valuable fine chemicals,[1-6] and it can get into the environment system during the above processes and pollute the nature water. The other source of p-nitrophenol in the environment is the hydrolysis or degradation of organic molecules containing p-nitrophenol moiety.[7] Therefore, p-nitrophenol has become a commonly encountered pollutant in water pollution nowadays. And it is known that p-nitrophenol has been categorized as one of the 126 priority pollutants by the U.S. Environmental Protection Agency (U.S. EPA) for its persistency, bioaccumulation and high toxicity even at very low concentration,[8-12] and frequent exposure to p-nitrophenol can cause methemoglobin formation, anemia, liver and kidney damage, eye and skin irritation, tumor formation, cancer, and systemic poisoning.[8, 9, 13, 14] Therefore, fast and effective removal of p-nitrophenol from industrial wastewater and nature water is becoming more and more urgent.

Several water treatment technologies have been developed with the aim to remove p-nitrophenol or its analogues from industrial wastewater and nature water effectively, such as adsorption,[4, 15-18] oxidation,[19-21] membrane separation,[22, 23] and extraction.[24] Among these technologies, adsorption is recognized as the most applicable one for its simple-design, easy-operation, and high-efficiency.[18, 25-27] And activated carbon is the most popular adsorbent employed in the adsorption process, for its large specific surface area and high adsorption capacity.[3, 4, 13, 17, 28] But as adsorbent, activated carbon also has its inherent limitations such as poor mechanical strength and difficult-regeneration.[3, 26, 28] So, there is an increasing interest in the research and development of adsorbent with satisfying adsorption capacity, high mechanical strength, high reusability, and ready availability, especially the adsorbent based on natural products for their ready

[a] College of Chemical Engineering, Zhejiang University of Technology, Hangzhou 310014, China.
[b] School of Chemistry and Chemical Engineering, Sun Yat-sen University, Guangzhou 510275, China
* Corresponding author. E-mail address: haimshen@zjut.edu.cn. Fax: (+86)571-8832-0533. Tel. : (+86)571-8832-0533.
Electronic Supplementary Information (ESI) available: [details of any supplementary information available should be included here]. See DOI: 10.1039/x0xx00000x

View Article Online
DOI: 10.1039/C5RA15592D

availability and excellent biocompatibility, which will not cause additional environmental pollution in their application.

β-Cyclodextrin (β-CD), is a water-soluble macrocyclic oligomer of D-(+)-glucopyranosyl units linked by α-1, 4-glycosidic bond, which possesses a hydrophilic exterior and a hydrophobic cavity. And β-CD can be readily available from the enzymatic degradation of starch, which makes it possessing excellent biocompatibility.[29-32] Because of its hydrophilic exterior and hydrophobic cavity, β-CD can form inclusion complexes with a wide range of organic molecules possessing suitable shape and size in water spontaneously,[33-36] which brings a possibility to remove the organic molecules from polluted water. Thus, β-CD has become a unique structural unit in the design and preparation of adsorbent employed in the water treatment.[37-44] In the water treatment process, β-CD unit can capture the pollutant molecules through formation of inclusion complexes effectively, and then the removal of the pollutant is realized through separation of the adsorbent from aqueous solution without any additional environmental pollution. But at present, in the immobilization of β-CD onto water-insoluble supporters such as Fe_3O_4,[40, 45-47] SiO_2,[48-50] graphene oxide,[51, 52] carbon nanotube,[53] and chitosan,[42, 54] linking groups mostly employed are epichlorohydrin,[42] citric acid,[48] carbodiimide,[46] 3-glycidyloxypropyl trimethoxysilane,[47] hexamethylene diisocyanate,[53] glutaraldehyde,[54] and so on. These linking groups possess so high reactivity that multiple hydroxyl groups in β-CD molecule may react with linking groups, which will weaken the intramolecular hydrogen bond in β-CD molecule, disfavour the maintenance of the hydrophobic cavity of β-CD and affect the adsorption performance, especially the adsorption rate, which is a very important property of adsorbent employed in fast adsorption.

Thus, in this work, β-CD was immobilized onto the surface of hybrid silica (Cl@Si), which was prepared through sol-gel hydrolysis-condensation of (3-chloropropyl)triethoxysilane (CPTES) and tetraethyl orthosilicate (TEOS) in the presence of tetrabutylammonium fluoride,[55-57] using ethylenediamine as linking groups to construct adsorbent in water treatment (CD@Si), in which only one hydroxyl group in the β-CD molecule was employed in order to maintain the hydrophobic cavity of β-CD. And the adsorbent was characterized by Fourier transform infrared spectroscopy (FT-IR), X-ray photoelectron spectroscopy (XPS), energy dispersive X-ray spectroscopy (EDX), contact angle measurement, thermo-gravimetric analysis (TGA), solid-state ^{13}C NMR, scanning electron microscopy (SEM), and X-ray diffraction (XRD). Then applied to the adsorption of p-nitrophenol from aqueous solution, CD@Si exhibits satisfying fast-adsorption performance, and adsorption equilibrium can be reached in 15 s with the equilibrium adsorption capacity of 69.6 mg/g, a very fast adsorption process. The effect of solution pH and contact time on the adsorption performance, adsorption kinetics, adsorption isotherms, adsorption thermodynamics, reusability and adsorption mechanism were also investigated systematically. It is demonstrated that CD@Si is a very suitable and promising adsorbent for fast adsorption in some cases of emergency. This work also provides a strategy to increase the adsorption rate of adsorbent based on β-CD.

2. Experimental section

2.1. Materials and chemicals

β-Cyclodextrin in 99% purity was purchased from Shanghai Bio Science & Technology Co. Ltd., China. p-Toluenesulfonyl chloride in 99% purity, and ethylenediamine in 99% purity were Shanghai Aladdin reagents. (3-Chloropropyl) triethoxysilane (CPTES) in 99% purity, orthosilicate (TEOS) in 99% purity, 1 M tetrabutylammonium fluoride in THF, p-nitrophenol in 99% purity, potassium dihydrogen phosphate (KH_2PO_4) in 99% purity and dipotassium hydrogen phosphate (K_2HPO_4) in 99% purity were purchased from Shanghai Energy Chemical Co. Ltd., China. Potassium iodide (KI) in 99% purity were purchased from Xilong Chemical Co. Ltd., China. Distilled water was used in all the experiments. All the other common reagents were analytical grade. All of the reagents were used as received without further purification unless otherwise noted.

2.2. Synthesis of mono[6-O-(p-toluenesulfonyl)]-β-CD

Mono[6-O-(p-toluenesulfonyl)]-β-CD was synthesized according to our procedure reported previously.[58-60] A solution of sodium hydroxide (6.00 g, 150 mmol) in water (20 mL) was added dropwise to a solution of β-CD (56.75 g, 50 mmol) in water (500 mL) with magnetic stirring at 10-15 °C over about 15 min. The solution became homogeneous, and then a solution of p-toluenesulfonyl chloride (11.44 g, 60 mmol) in acetonitrile (30 mL) was added dropwise at 10-15 °C over about 45 min forming white precipitate immediately. The resultant solution was kept stirring for 3.0 h and rose to room temperature. The precipitate formed was obtained by suction filtration and then suspended in water (300 mL) with magnetic stirring at room temperature for 3.0 h. The precipitate collected by suction filtration was washed successively with acetone (100 mL) and water (160 mL), and then dried in vacuum at 80 °C for 8.0 h to afford white solid powder 8.17 g in 12.67% yield. $[\alpha]_D^{25}$ = +124.15° (c = 0.8044, DMF); m.p. > 160 °C (decomp.); ^1H NMR (400 MHz, DMSO-d_6): δ = 7.76 (d, J = 8.3 Hz, 2H), 7.44 (d, J = 8.2 Hz, 2H), 5.83-5.63(m, 14H), 4.85-4.76 (m, 7H), 4.50-4.44 (m, 5H), 4.37-4.32 (m, 2H), 4.21-4.17 (m, 1H), 3.70-3.43 (m, 26H), 3.40-3.19 (m, 14H, overlaps with H_2O), 2.43 ppm (s, 3H); ^{13}C NMR (400 MHz, DMSO-d_6): δ = 144.67, 132.53, 129.75, 127.44, 102.09-101.14 (m), 81.51-80.63 (m), 72.88-71.69 (m), 69.56, 68.76, 59.74-59.04 (m), 21.06 ppm; MS (ESI): m/z: 1311.3 $[M+Na]^+$, 1289.0 $[M+H]^+$. The modification of β-CD with p-toluenesulfonyl chloride to construct mono[6-O-(p-toluenesulfonyl)]-β-CD is the first step to activate the hydroxyl of β-CD, which produces an important intermediate in the preparation of adsorbent CD@Si.

2.3. Synthesis of mono(6-ethylenediamine)-β-CD

A solution of mono[6-O-(p-toluenesulfonyl)]-β-CD (6.45 g, 5.0 mmol) in ethylenediamine (22.54 g, 375 mmol) was stirred at

View Article Online
DOI: 10.1039/C5RA15592D

70 °C for 24.0 h, and then cooled to room temperature. The resultant solution was poured into ethanol (400 mL) slowly forming white precipitate immediately. The white precipitate was collected by suction filtration and dried in vacuum at 80 °C for 8.0 h. Then obtained white power was recrystallized two times in water (2×10 mL), dried in vacuum at 80 °C for 8.0 h to afford white crystal 3.18 g in 54.03% yield. $[\alpha]_D^{25}$ = +149.91° (c = 0.8036, H_2O); m.p. > 245 °C (decomp.); ^{1}H NMR (400 MHz, D_2O): δ = 5.12-5.10 (m, 7H), 4.03-3.89 (m, 26H), 3.70-3.59 (m, 14H), 3.48 (t, J = 9.4 Hz, 1H), 3.11-3.08(m, 1H), 2.87-2.68 ppm (m, 7H); ^{13}C NMR (400 MHz, D_2O): δ = 101.81, 100.47, 83.56, 81.09, 80.86, 73.06-72.96 (m), 72.05-71.99 (m), 71.78, 70.42, 60.25, 50.66, 49.29, 42.19, 39.73 ppm; MS (ESI): m/z: 1177.5 $[M+H]^+$. Mono(6-ethylenediamine)-β-CD which can be immobilized onto the surface of hybrid silica (Cl@Si) directly, is the second important intermediate in the preparation of adsorbent CD@Si.

2.4. Preparation of hybrid silica (Cl@Si)

Cl@Si was prepared according to the literature procedure with some modification.[55-57] A solution of (3-chloropropyl) triethoxysilane (CPTES) (2.41g, 10 mmol), orthosilicate (TEOS) (10.42g, 50 mmol) in anhydrous ethanol (30 mL) was added to a solution of distilled water (3.60g, 200 mmol), 1 M tetrabutylammonium fluoride in THF (3.0 mL) in anhydrous ethanol (20 mL). The resultant mixture was shaken vigorously for 5 s to obtain a homogenous solution and was then kept under static conditions. After 30 min, gelification was observed, and the material was aged at room temperature for 6 days. The obtained gel was pulverized, separated by filtration and washed successively with ethanol (3×50 mL) and acetone (2×50 mL). The resultant solid was dried in vacuum at 80 °C for 24.0 h to afford water-insoluble supporter Cl@Si as white power 4.46 g.

2.5. Preparation of β-CD immobilized on Cl@Si (CD@Si)

To a solution of mono(6-ethylenediamine)-β-CD (18.00 g), KI (0.30 g) in dry N,N-dimethylformamide (360 mL), Si@Cl (12.00 g) was added, and the reaction mixture was heated to 110 °C and kept stirring for 72.0 h under nitrogen atmosphere. After cooling to room temperature, the suspension was filtered and the obtained solid was washed successively with N,N-dimethylformamide (100 mL), ethanol (3×200 mL) and water (2×200 mL). The resultant solid was dried in vacuum at 80 °C for 24.0 h to afford CD@Si as white power 12.30 g.

The preparation procedure of CD@Si is illustrated in **Scheme 1.**

2.6. Characterization

FT-IR spectra of Cl@Si and CD@Si were record on a Nicolet 6700 spectrometer using KBr as background over the frequency range of 4000~400 cm^{-1}. XPS analysis was carried out on a Kratos AXIS Ultra DLD spectrometer with Al mono Kα X-ray source (1486.71 eV photons) to investigate the elementary distribution on the surface of Cl@Si and CD@Si. EDX analysis was carried out on the Philips-FEI Tecnai G2 F30 S-Twin transmission electron microscope to investigate the elementary composition of Cl@Si and CD@Si. Contact angle measurements were conducted through dropping water droplets (6 μL) on the surface of Cl@Si and CD@Si respectively, and after waiting for 30 s to let the water droplets on the surface of Cl@Si and CD@Si become stable, the KRÜSS DSA100 Drop Shape Analysis System was employed to measure the contact angel and determine their hydrophobicity / hydrophilicity level. The TGA were carried out under nitrogen atmosphere from room temperature to 800 °C at a speed of 10 °C/min employing a STA 449 F3 Jupiter® spectrometer to monitor the weight loss of Cl@Si and CD@Si, and to determine the immobilized amount of β-CD on the surface of hybrid silica. The solid state NMR (^{13}C CP MAS) data of Cl@Si and CD@Si was collected using BRUKER AVANCE II 300MHZ spectrometer to determine the successful immobilization of β-CD on the surface of hybrid silica. The morphologies of Cl@Si and CD@Si were observed by SEM (Hitachi S-4700 (II) instrument). The XRD patterns were recorded on a X' Pert PRO X-ray diffractometer with a Cu Kα radiation (λ = 1.5418Å) in the range of 5~60º.

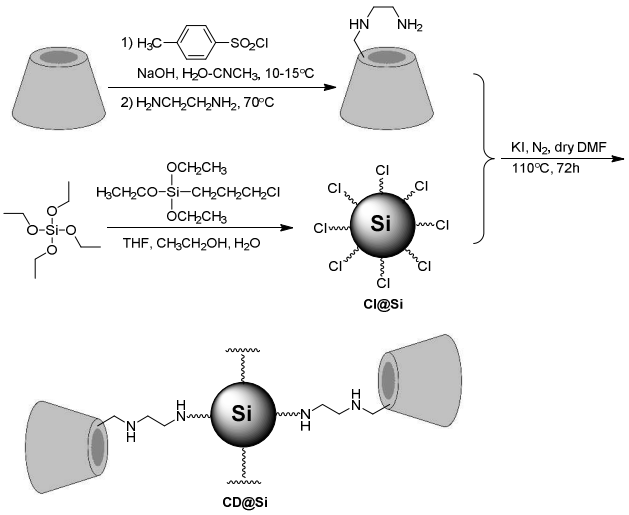

Scheme 1 The schematic preparation of CD@Si.

2.7. Adsorption experiment

Batch experiments were carried out to investigate the adsorption performance of adsorbent CD@Si to p-nitrophenol because of the simplicity and reliability of this method. In experiments, CD@Si (0.10 g) was added to a 25-mL glass conical flask placed in a thermostatic water-bath shaking incubator at 283K, 293K, 303K and 313K respectively, and then aqueous solution of p-nitrophenol (10.0 mL) in the initial concentration of 0.10 g/L, 0.50 g/L, 1.00 g/L, 1.50 g/L, 2.00 g/L, 2.50 g/L, 3.00 g/L and 4.00 g/L, and at 283K, 293K, 303K and 313K was added, respectively. After shaking at 150 rpm for 2.0 h, the suspensions was poured into distilled water (90 mL) quickly to weaken the further adsorption and 10 mL of the upper liquid was filtered through 0.45 μm filter membrane quickly to remove the adsorbent residue. The concentration of p-nitrophenol in the filtrate was detected on a UV-vis

View Article Online
DOI: 10.1039/C5RA15592D

spectrophotometer (Shimadzu, UV-2250) at wavelength of 398 nm. In order to investigate the effect of the solution pH, KH_2PO_4-K_2HPO_4 buffer solution was employed. In the experiments to determine the effect of temperature, the aqueous solution of p-nitrophenol was held at 283K, 293K, 303K and 313K respectively, and the adsorption experiments were also performed at above temperature. Each experiment was carried out twice, and the experiment data are the average values. The amount of p-nitrophenol adsorbed onto CD@Si was calculated according the following equation:

$$q_t = \frac{(C_0 - C_t) \times V}{m} \quad (1)$$

where q_t is the adsorption capacity (mg/g) at time t, C_0 is the initial concentration of p-nitrophenol (g/L), C_t is the concentration of p-nitrophenol (g/L) at time t (s), V is the volume of the aqueous solution of p-nitrophenol (mL), m is the mass of adsorbent CD@Si (g) employed.[5, 18, 37] Thus the equilibrium adsorption amount was calculated according the following equation:

$$q_e = \frac{(C_0 - C_e) \times V}{m} \quad (2)$$

where q_e is the equilibrium adsorption capacity (mg/g), C_0 is the initial concentration of p-nitrophenol (g/L), C_e is the equilibrium concentration of p-nitrophenol (g/L), V is the volume of the aqueous solution of p-nitrophenol (mL), m is the mass of adsorbent CD@Si (g) employed.[5, 18, 37]

2.8. Data analysis

2.8.1. Adsorption kinetics

In kinetic study, two kinetic models, pseudo-first-order and pseudo-second-order models were employed to analysis the experimental data and predict the adsorption kinetics in this work. The linear form of equation for the pseudo-first-order model is described as following:

$$\ln(q_e - q_t) = \ln q_e - k_1 t \quad (3)$$

where q_e and q_t are the adsorption amount of p-nitrophenol on CD@Si (mg/g) at equilibrium and at time t, respectively, and k_1 is the pseudo-first-order adsorption rate constant (s^{-1}).[18, 39, 61]

The linear form of equation for the pseudo-second-order model is expressed as following:

$$\frac{t}{q_t} = \frac{1}{k_2 q_e^2} + \frac{t}{q_e} \quad (4)$$

where q_e and q_t are the same as in the pseudo-first-order model, and k_2 is the pseudo-second-order adsorption rate constant (g/(mg·s)).[18, 39, 61]

2.8.2. Adsorption isotherm

In adsorption isotherm study, Langmuir, Freundlich and Tempkin models were employed. The linear form of equation for the Langmuir model is described as following:

$$\frac{C_e}{q_e} = \frac{1}{K_L q_m} + \frac{C_e}{q_m} \quad (5)$$

where C_e is the equilibrium concentration of p-nitrophenol in the aqueous solution (g/L), q_e is the equilibrium adsorption capacity (mg/g), q_m is the maximum adsorption capacity (mg/g), and K_L is the equilibrium adsorption constant (L/g).

The Freundlich model can be expressed in the linear form as following:

$$\ln q_e = \ln K_F + \frac{1}{n} \ln C_e \quad (6)$$

where q_e and C_e are the same as in Langmuir model, K_F (L/g) and n are the Freundlich constants.[37, 39]

The Tempkin model can be expressed in the linear form as following:

$$q_e = k_1 \ln k_2 + k_1 \ln C_e \quad (7)$$

where k_1 is the Tempkin constant related to the adsorption heat (L/g), k_2 is the Tempkin isotherm constant.[1, 14, 62]

2.8.3. Adsorption thermodynamics

In order to investigate the effect of temperature on the adsorption process, thermodynamic parameters containing Gibbs free energy change (ΔG), enthalpy change (ΔH) and entropy change (ΔS) were determined employing the following equation:

$$\Delta G = -RT \ln K_d \quad (8)$$

$$\Delta G = \Delta H - T\Delta S \quad (9)$$

$$\ln K_d = \frac{\Delta S}{R} - \frac{\Delta H}{RT} \quad (10)$$

$$K_d = \frac{q_e}{C_e} \quad (11)$$

where K_d is the distribution coefficient, R (8.314 J·mol^{-1}·K^{-1}) is the universal gas constant, and T is Kelvin temperature (K).[6, 14, 63-65] ΔH and ΔS can be obtained from the slope and intercept of the plots of lnK_d versus 1/T, thus ΔG was obtained employing equation (9).

2.9. Reusability of CD@Si

CD@Si (0.30 g) was added to a 100-mL glass conical flask placed in a thermostatic water-bath shaking incubator at 303 K, and then aqueous solution of p-nitrophenol (30.0 mL) in 2.0 g/L and pH 7.0 was added. After shaking at 150 rpm for 2.0 h, the suspensions was centrifuged at 4500 rpm for 10.0 min. The upper liquid was filtered through 0.45 μm filter membrane quickly to remove the adsorbent residue. The concentration of p-nitrophenol in the filtrate was detected on a UV-vis spectrophotometer (Shimadzu, UV-2250) at wavelength of 398 nm to determined the amount of p-nitrophenol adsorbed onto CD@Si.The obtained solid was washed successively with enthanol (3 × 10 mL) and water (3 × 10 mL) under ultrasonic and centrifugal condition, and then dried in vacuum at 80 °C for 8.0 h. Then the regenerated CD@Si was subjected to the second run under the same adsorption conditions, and for the loss of adsorbent in the reusability experiment, the volume of p-nitrophenol aqueous solution added should be decreased proportionally.

View Article Online
DOI: 10.1039/C5RA15592D

3. Results and discussion

3.1. Characterization

The FT-IR spectra of Cl@Si, CD@Si, and β-CD are presented in **Fig. 1**. The strong and broad peaks at around 3380 cm^{-1} are attributed to the O-H stretching vibrations, the peaks at around 2900 cm^{-1} belong to the C-H stretching vibrations and the peaks at around 1650 cm^{-1} are the N-H deformation vibrations in secondary amine. Comparing the FT-IR spectrum of CD@Si with Cl@Si, the O-H stretching vibration in CD@Si become stronger for the abundant hydroxyl groups existing in β-CD molecule, and the difference of C-H stretching vibration at around 2900 cm^{-1} is not very obvious. When β-CD was immobilized onto the surface of Cl@Si, the N-H deformation vibration at around 1650 cm^{-1} appeared in CD@Si for the existence of secondary amine groups. And the not obvious peak at around 1650 cm^{-1} appeared in the spectrum of Cl@Si mainly comes from the bending vibrations of a little adsorbed water, not the N-H deformation vibrations in amine groups. Thus, it can be concluded from the FT-IR spectra that β-CD have been immobilized on the surface of hybrid silica successfully. Another strong evidence for the successful immobilization of β-CD on the surface of hybrid silica is the XPS and EDX spectra as shown in **Fig. 2**. Compared with Cl@Si, in the XPS spectrum of CD@Si, chlorine element decreased and nitrogen element was detected for the nucleophilic substitution reaction between nitrogen atoms and chlorine atoms. The similar elementary change was also observed in the EDX spectra of Cl@Si and CD@Si.Both the XPS analysis and the DEX analysis are very direct evidences for the successful immobilization of β-CD on the surface of hybrid silica. The successful immobilization of β-CD on the surface of hybrid silica was also illustrated by the contact angle measurement in **Fig.3**. The surface of Cl@Si is hydrophobic for the existence of hydrophobic -$CH_2CH_2CH_2Cl$, so the contact angle of water on it can reach up to 143.6º. But the surface of CD@Si is hydrophilic for the existence of massive -OH, so water droplet (6 μL) on the surface of CD@Si can seep into it quickly (within 30 s) as shown in **Fig.3** (b). So the contact angle measurement is also a very visual evidence for the successful immobilization of β-CD on the surface of hybrid silica. Solid state CP MAS ^{13}C NMR analysis of Cl@Si and CD@Si was also conducted to characterize the successful immobilization as shown in **Fig.4**. The broad signals from 55.5 to 6.5 in **Fig.4** (a) belong to the carbon atoms in CPTES on the surface of hybrid silica (Cl@Si). The broad signals from 160.9 to 5.8 in **Fig.4** (b) are attributed to the carbon atoms in CPTES and β-CD. Thus, from the systematic characterization above, it is confirmed that β-CD has been immobilized onto the surface of hybrid silica successfully.

The amount of β-CD immobilized on the surface of hybrid silica was evaluated through TGA spectra of Cl@Si and CD@Si under the atmosphere of nitrogen. As shown in **Fig.5**, the total weight loss of Cl@Si over the full temperature range is about 19% for the evaporation of adsorbed water on the surface of Cl@Si, dehydration of the hydroxyl groups on the surface, and thermal decomposition of CPTES moieties. Before 250 ºC, the weight loss is about 2 % because the surface of Cl@Si is hydrophobic and no water can be adsorbed on its surface. In the range of 250 ºC to 800 ºC, the weight loss of Cl@Si is about 17 %, which is mainly contributed to the thermal decomposition of CPTES moieties. Thus, the organic layer on hybrid silica (Cl@Si) is about 17%. As for CD@Si, the weight

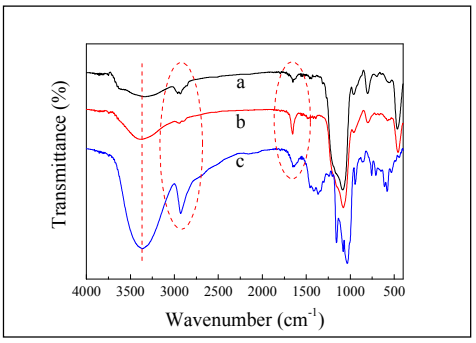

Fig. 1 FT-IR spectra of (a) Cl@Si, (b) CD@Si, and (C) β-CD.

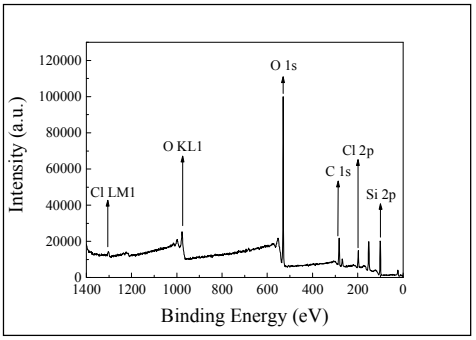

a

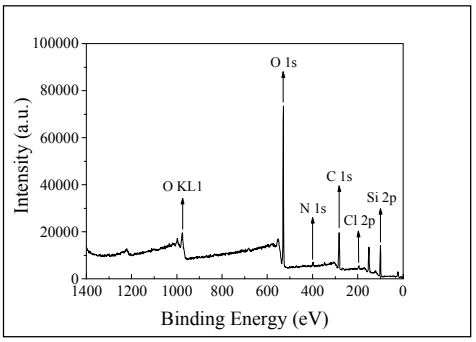

b

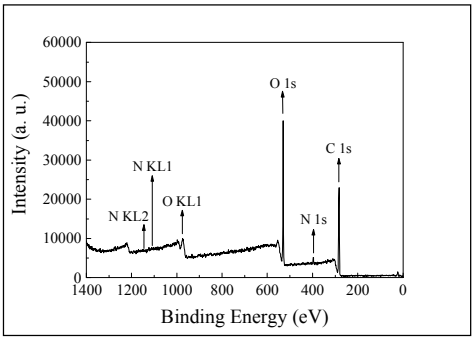

c

View Article Online
DOI: 10.1039/C5RA15592D

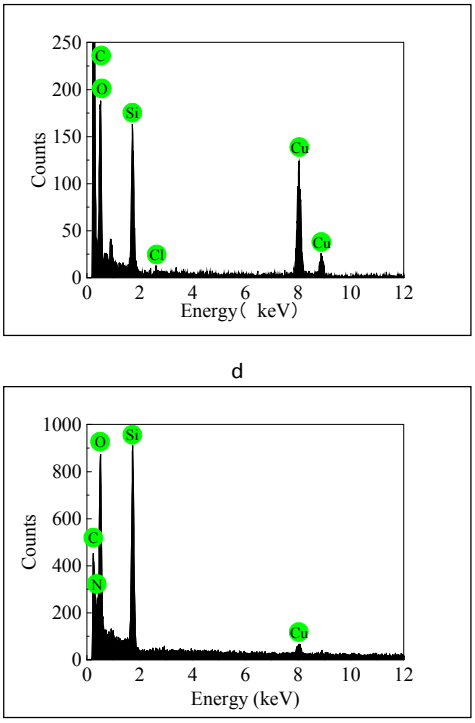

Fig. 2 XPS spectra of (a) Cl@Si, (b) CD@Si, (C) β-CD and EDX spectra of (d) Cl@Si, (e) CD@Si.

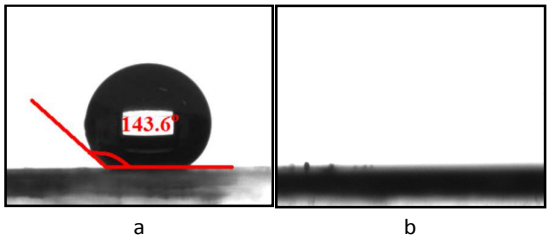

Fig. 3 Contract angles of water on (a) Cl@Si, and (b) CD@Si.

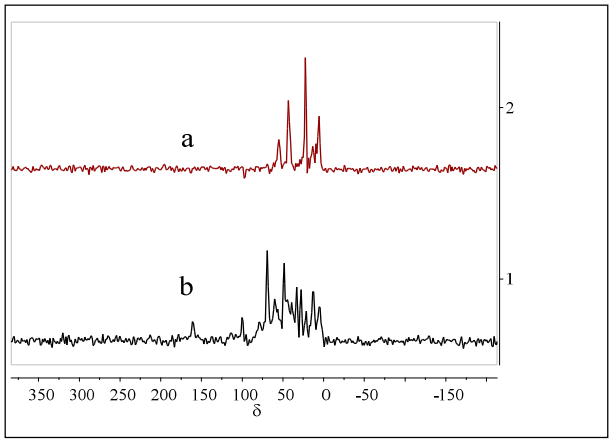

Fig. 4 Spectra of solid state CP MAS ^{13}C NMR of (a) Cl@Si, and (b) CD@Si.

loss before 150 ºC is about 3% for the evaporation of adsorbed water on the surface of CD@Si and the included water in the cavity of β-CD. In the range of 150 ºC to 800 ºC, the weight loss of CD@Si is about 25%, which is contributed to the thermal decomposition of β-CD moieties and $-CH_2CH_2CH_2-$ moieties. Thus, the amount of β-CD immobilized on the surface of hybrid silica is about 25% (m/m) with omitting of the mass contribution of $-CH_2CH_2CH_2-$ moieties. The TGA curves also provide a further evidence for the successful immobilization of β-CD on the surface of hybrid silica.

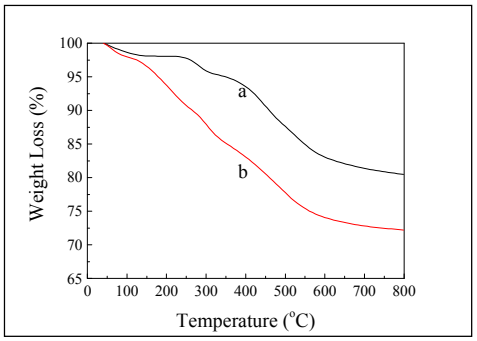

Fig. 5 TGA curves of (a) Cl@Si, and (b) CD@Si.

The morphologies of Cl@Si and CD@Si were analyzed by SEM as shown in **Fig.6**. It is obvious that their morphologies are uniform in both shape and size, and the immobilization of β-CD on the surface of hybrid silica did not affect the morphology of hybrid silica. And the morphological differences between Cl@Si and CD@Si are not very significant. The XRD patterns of Cl@Si, CD@Si and β-CD were listed in **Fig.7**, in which both of Cl@Si and CD@Si exhibit a broad peak centered at about 22º which is the characteristic peak of SiO_2.[66] Thus, the hybrid silica we prepared was confirmed as SiO_2, and in the immobilization process of β-CD, the original structure of hybrid silica had not been changed. The lost of the β-CD's characteristic peaks when β-CD is immobilized onto Cl@Si, is mainly attributed to the monolayer distribution of β-CD on the surface of Cl@Si. And in the monomolecular layer of β-CD, there are not enough molecules to form β-CD crystals, so the β-CD's characteristic peaks in XRD measurement can not be observed.

From the systematic characterization above, it is confirmed that β-CD has been immobilized onto the surface of hybrid silica successfully, and the immobilization process did not affect the original structure of hybrid silica.

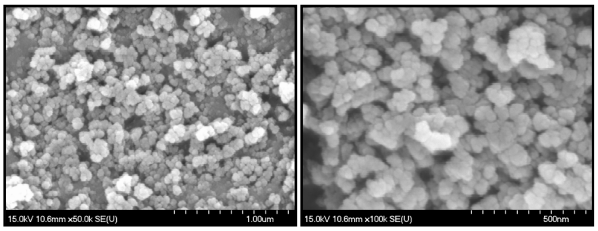

a

View Article Online
DOI: 10.1039/C5RA15592D

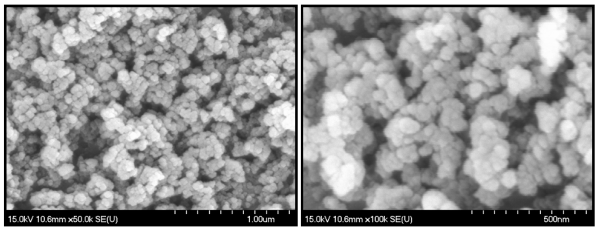

b

Fig. 6 SEM images of (a) Cl@Si, and (b) CD@Si.

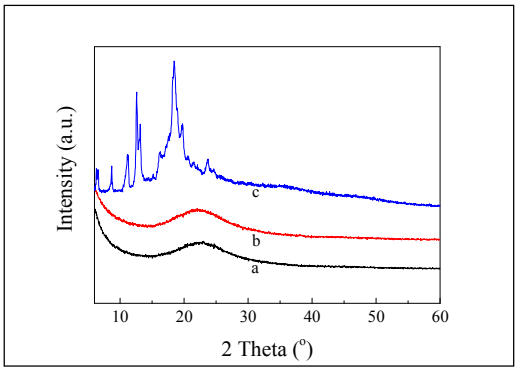

Fig. 7 XRD patterns of (a) Cl@Si, (b) CD@Si, and (C) β-CD.

3.2. Effect of solution initial pH on the adsorption capacity

The adsorption of p-nitrophenol from aqueous solution by CD@Si is influenced significantly by the pH value of the solution, because pH not only affects the protonation of adsorbent CD@Si, but also plays a crucial role in the ionization of p-nitrophenol.[18, 67] Thus, the effect of solution pH on the adsorption performance of CD@Si to p-nitrophenol was investigated systematically in the pH range of 5.0 to 10.0. As shown in **Fig. 8**, with the increase of solution pH from 5.0 to 7.0, the adsorption capacity increased from 8.9 to 15.2 mg/g, 19.6 to 40.4 mg/g, 27.5 to 53.7 mg/g, and 34.3 to 69.6 mg/g in the initial concentration of 0.50, 2.00, 3.00, and 4.00 g/L, respectively. Further increase in the solution pH leads to a slight decrease in the adsorption capacity. The above profile of adsorption capacity to pH is explained as following: in this adsorption system, the adsorption capacity contains two parts: inclusion in the hydrophobic cavity of β-CD and hydrogen bond interaction between β-CD unit on CD@Si and p-nitrophenol, and in the acidic condition, both β-CD unit on CD@Si and p-nitrophenol become protonated, so p-nitrophenol can not be adsorbed onto CD@Si efficiently for the electrostatic repulsion between them. And when pH increased, both the protonation of CD@Si and p-nitrophenol became weak, so the adsorption capacity increased, which could be attributed to the hydrogen bond interaction between β-CD unit on CD@Si and p-nitrophenol. In the neutral condition, the protonation of adsorbent CD@Si and p-nitrophenol disappears, and the hydrogen bond interaction between them favours the adsorption of p-nitrophenol onto CD@Si. In the basic condition, the ionization of p-nitrophenol occurs, which brings about the electrostatic repulsion between p-nitrophenol molecules, weakens the adsorption of p-nitrophenol on the surface of CD@Si as multi-layer molecules. Thus the adsorption capacity reaches its maximum in pH 7.0. Therefore, it is concluded that the adsorption of p-nitrophenol by CD@Si is a pH-dependent process, and in the neutral condition (pH 7.0), CD@Si can reach its optimal adsorption performance.

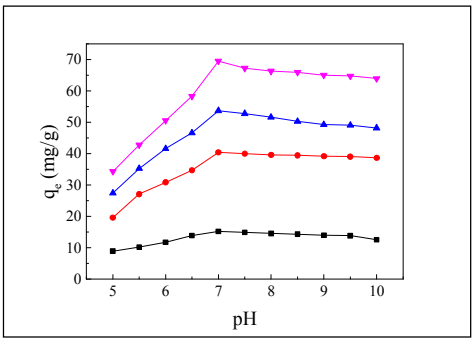

Fig. 8 Effect of solution initial pH on the adsorption of p-nitrophenol by CD@Si.
Conditions: Initial concentration of p-nitrophenol, ■ 0.50 g/L, ● 2.00 g/L, ▲ 3.00 g/L, ▼ 4.00 g/L in 0.05 mol/L KH_2PO_4-K_2HPO_4 buffer solution. Solution volume of p-nitrophenol, 10.0 mL. Adsorbent CD@Si, 0.10 g. Shaking speed, 150 rpm. Temperature, 303 K. Contact time, 2.0 h.

3.3. Effect of contact time on the adsorption capacity

The objective of our study is to develop an adsorbent with high adsorption rate and satisfying adsorption capacity for p-nitrophenol and its analogues based on β-CD, so the adsorption equilibrium time and the equilibrium adsorption capacity are two major parameters investigated in this work. The profiles of adsorption capacity to contact time in the initial concentration of 1.00, 2.00, 3.00, and 4.00 g/L were presented in **Fig.9**, and what should be mentioned here is that in our work, in order to eliminate the effect of adsorption during the separation process of CD@Si from the adsorption system, after shaking for a certain time, the suspensions (10 mL) was poured into distilled water (90 mL) quickly to weaken the further adsorption. Then 10 mL of the upper liquid was filtered through 0.45 μm filter membrane quickly to remove the adsorbent residue. As shown in **Fig. 9**, the adsorption equilibrium in the adsorption of p-nitrophenol by CD@Si can be obtained within only 15 s for various initial concentrations, a very fast adsorption process, and the initial concentration of p-nitrophenol does not have any significant effect on the adsorption rate. It is also observed from **Fig.9** that, with the increase in the initial concentration, the equilibrium adsorption capacity increased, because both the inclusion process between p-nitrophenol and β-CD unit, and the hydrogen bond interaction between p-nitrophenol and β-CD unit on CD@Si are reversible, high initial concentration favours p-nitrophenol adsorbed onto the surface of CD@Si.

In order to further verify the fast adsorption performance of CD@Si to p-nitrophenol, the performance of some reported adsorbents based on β-CD in the adsorption of p-nitrophenol

View Article Online
DOI: 10.1039/C5RA15592D

or its analogues were listed in **Table 1** for comparison. In **Table 1**, it is obvious that the equilibrium adsorption capacity of CD@Si is not the most satisfying one, but considering the time needed to reach adsorption equilibrium, CD@Si is the most promising one, because the adsorption equilibrium can be achieved within 15 s with an acceptable equilibrium adsorption capacity, 69.6 mg/g, which is the highest adsorption capacity per unit time for the above adsorbent listed in **Table 1**. Thus, it is very suitable to apply CD@Si to some cases of emergency needing fast adsorption such as the leakage of p-nitrophenol in a large amount to nature water. In that case, to prevent p-nitrophenol from diffusing with the flow of water quickly is the first issue needed to be taken into consideration, and the maximum removal of p-nitrophenol in unit time is the most efficient strategy. Therefore, the prepared adsorbent CD@Si in this work is a very attractive choice in the fast adsorption of p-nitrophenol. The fast adsorption performance is mainly attributed to the maintenance of the hydrophobic cavity of β-CD for only one hydroxyl group in the β-CD molecule was employed in the preparation of CD@Si. And the distribution of β-CD unit on the surface of hybrid silica is another important reason for the fast adsorption because no diffusion resistance exists. When CD@Si enters into the aqueous solution of p-nitrophenol, p-nitrophenol molecules transfer from the solution into the hydrophobic cavity of β-CD unit and onto the surface of β-CD layer quickly, thus adsorption equilibrium is obtained within only 15 s with acceptable adsorption capacity.

By comparing the adsorption capacity of CD@Si (69.6mg/g) with Cl@Si (5.8 mg/g), we also can obtain that, in the adsorbent CD@Si, the adsorption function mainly comes from the β-CD unit. The adsorption capacity of Cl@Si to p-nitrophenol is in a negligible level. The poor adsorption performance of Cl@Si is mainly because of its hydrophobicity, which can not be dispersed well in aqueous solution at all. The above experimental phenomenon demonstrates the importance of β-CD unit in the construction of adsorbent too, especially the one applied in aqueous solution.

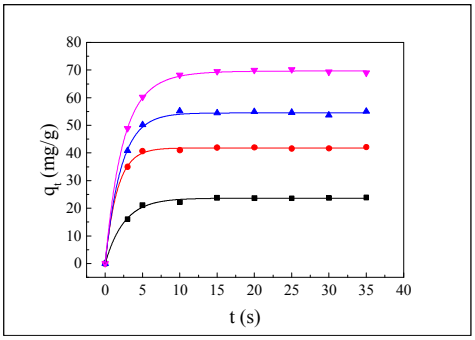

Fig. 9 Effect of contact time on the adsorption of p-nitrophenol by CD@Si.
Conditions: Initial concentration of p-nitrophenol, ■1.00 g/L, ● 2.00 g/L, ▲3.00 g/L, ▼4.00 g/L in 0.05 mol/L KH_2PO_4-K_2HPO_4 buffer solution. Initial pH of solution, 7.0. Solution volume of p-nitrophenol, 10.0 mL. Adsorbent CD@Si, 0.10 g. Shaking speed, 150 rpm. Temperature, 303 K.

Table 1 Comparison of some reported adsorbents based on β-CD in the adsorption of p-nitrophenol or its analogues.

NO	Adsorbent	Solute	Equilibrium Time	Equilibrium Adsorption (mg/g)
1	CD@Si	p-Nitrophenol	15 s	69.6
2	Cl@Si	p-Nitrophenol	15 s	5.8
3[67]	β-CD-Zeolite	p-Nitrophenol	60 min	0.3
4[2]	β-CD-Carbon nanotube-Fe_3O_4	p-Nitrophenol	180 min	33.3
5[68]	β-CD-Chitosan -Fe_3O_4	Hydroquinol	50 min	192.7
6[69]	β-CD-Attapulgite	2,6-Dichlorophenol	100 min	58.1
7[69]	β-CD-Attapulgite	2,6-Dichlorophenol	100 min	55.2
8[70]	β-CD-Poly(4-vinylbenzyl chloride)	2-Chlorophenol	180 min	61.7
9[71]	β-CD Polymer	Phenol	300 min	29.0
10[42]	β-CD-Chitosan	4-Chlorophenol	60 min	35.7

3.4. Adsorption kinetics

The adsorption capacity of CD@Si to p-nitrophenol versus contact time has been illustrated in **Fig.9** in the initial concentration of 1.00, 2.00, 3.00, and 4.00 g/L at 303 K. It is obvious that the adsorption is a very fast process and the adsorption equilibrium can be obtained within only 15 s with acceptable adsorption capacity. In order to further investigate this adsorption process and the adsorption mechanism, two kinetic models, pseudo-first-order and pseudo-second-order models were employed to analysis the adsorption kinetics of p-nitrophenol onto CD@Si following the Equ. (3) and (4). The plots of $\ln(q_e-q_t)$ versus t (pseudo-first-order model) and t/q_t versus t (pseudo-second-order model) in the initial concentrations of 1.00, 2.00, 3.00, and 4.00 g/L are presented in **Fig. 10**. It is very clear that the pseudo-second-order model fits the adsorption kinetic of p-nitrophenol onto CD@Si well with high correlation coefficient (R^2 >99%). As for the pseudo-first-order model, a liner relationship between $\ln(q_e-q_t)$ and t can not be obtained, meaning that the pseudo-first-order model can not describe the adsorption kinetic in this work. The pseudo-second-order kinetic model also was confirmed through the similar values of the experimental equilibrium adsorption capacity $q_{e,exp}$ and the calculated ones $q_{e,cal}$ as shown in **Table 2**. The experimental equilibrium adsorption capacity $q_{e,exp}$ are 23.7, 40.4, 53.7, and 69.6 mg/g, and meanwhile the calculated ones $q_{e,cal}$ are 24.7, 42.5, 55.7 and

View Article Online
DOI: 10.1039/C5RA15592D

71.5 mg/g in the initial concentration of 1.00, 2.00, 3.00, and 4.00 g/L respectively, a very good consistency with tiny error. The statistical errors in the adsorption kinetic study are mainly attributed to the errors in the weight of adsorbent CD@Si and solute p-nitrophenol, and in the preparation of aqueous solution of p-nitrophenol. Another origin of the statistical error is the systematic error in the UV measurement. The pseudo-second-order kinetic also suggests that in the adsorption of p-nitrophenol onto CD@Si, the rate-limiting step may involve valence forces through electrons sharing or exchange between p-nitrophenol and CD@Si such as hydrogen bond,[72, 73] which has been mentioned above. The pseudo-second-order adsorption mechanism is the predominant mechanism in the adsorption of p-nitrophenol onto CD@Si.

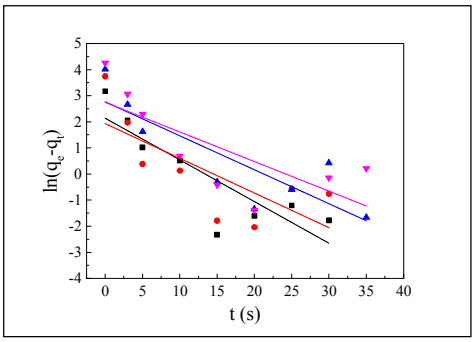

a

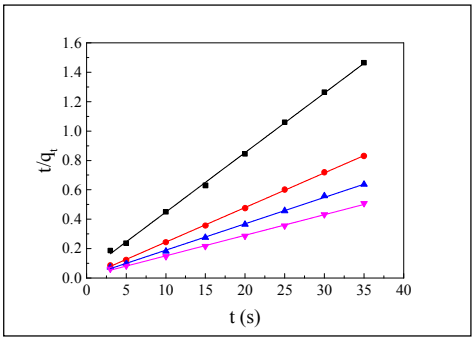

b

Fig. 10 Pseudo-first-order model (a) and Pseudo-second-order model (b) fits for the adsorption of p-nitrophenol by CD@Si. Conditions: Initial concentration of p-nitrophenol, ■1.00 g/L, ● 2.00 g/L, ▲3.00 g/L, ▼4.00 g/L in 0.05 mol/L KH_2PO_4-K_2HPO_4 buffer solution. Initial pH of solution, 7.0. Solution volume of p-nitrophenol, 10.0 mL. Adsorbent CD@Si, 0.10 g. Shaking speed, 150 rpm. Temperature, 303 K.

Table 2 The pseudo-first-order and pseudo-second-order kinetic parameters for the adsorption of p-nitrophenol by CD@Si at 303K.

C_0 (g/L)	$q_{e,exp.}$ (mg/g)	Pseudo-first-order			Pseudo-second-order		
		$q_{e1,\,cal}$ (mg/g)	$k_1\times10^{-2}$ (1/s)	R^2	$q_{e2,\,cal}$ (mg/g)	$k_2\times10^{-2}$ (g/(mg·s))	R^2
1.00	23.7	8.484	15.97	0.7058	24.7	3.776	0.9992
2.00	40.4	6.886	13.29	0.4845	42.5	6.327	0.9997
3.00	53.7	15.87	13.01	0.6742	55.7	3.272	0.9988
4.00	69.6	15.56	11.34	0.4888	71.5	1.753	0.9987

3.5. Adsorption isotherms

In order to further understand the adsorption mechanism, the adsorption isotherms of CD@Si to p-nitrophenol at four different temperature (283K, 293K, 303K, and 313K) were measured, which is an important illustration of how the adsorbate interacts with the adsorbent in equilibrium state. From the study of adsorption isotherms, the maximum adsorption capacity of CD@Si to p-nitrophenol also can be obtained. Several adsorption isotherm models have been developed to fit the adsorption data. In this work, three isotherm models, Langmuir model, Freundlich model and Tempkin model, were employed, which can be expressed linearly following Equ. (5), Equ. (6) and Equ. (7). For the Langmuir model, the basic theory assumption is that all the adsorption sites on the adsorbent surface are homogeneous, having equal affinity to the adsorbate molecules, and the occupation of one adsorption site do not have any effect on the performance of adjacent adsorption site. In Langmuir adsorption model, the adsorbate molecules usually form a monomolecular layer on the surface of adsorbent.[5, 74] For the Freundlich model, the basic theory assumption is that the distribution of adsorption sites on the adsorbent surface are heterogeneous, the stronger adsorption sites are occupied firstly, and with the increase in the coverage of adsorbent surface, the affinity of adsorbent to adsorbate decreases.[5, 74] For adsorbent with heterogeneous surface, Freundlich model is closer to the reality than Langmuir model. For the Tempkin model, the basic theory assumption is that in the adsorption process, the distribution of adsorption energy is uniform, and the adsorption energy decreases linearly as the increase in the adsorbent coverage.[1, 62]

The adsorption isotherm fitting was conducted employed Equ. (5), Equ. (6) and Equ. (7) for Langmuir model, Freundlich model and Tempkin model respectively. The plots of C_e/q_e versus C_e (Langmuir model), $\ln q_e$ versus $\ln C_e$ (Freundlich model), and q_e versus $\ln C_e$ (Tempkin model) at 283K, 293K, 303K, and 313K are presented in **Fig. 11**. The initial concentrations of p-nitrophenol in the adsorption isotherm study are 0.10, 0.50, 1.00, 1.50, 2.00, 2.50, 3.00, and 4.00g/L. And the adsorption isotherm parameters were summarized in **Table 3** which were obtained from the slope and intercept of the linear plots. It is very obvious that the Freundlich model with high correlation coefficient (R^2 >98%) in all the temperature involved fits the adsorption data better than

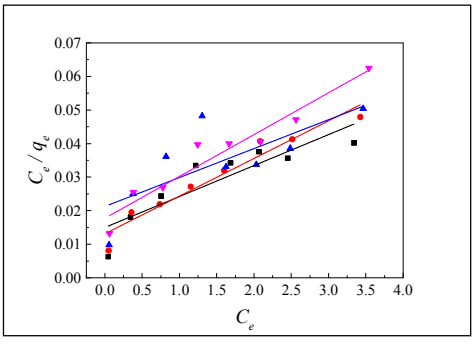

a

View Article Online
DOI: 10.1039/C5RA15592D

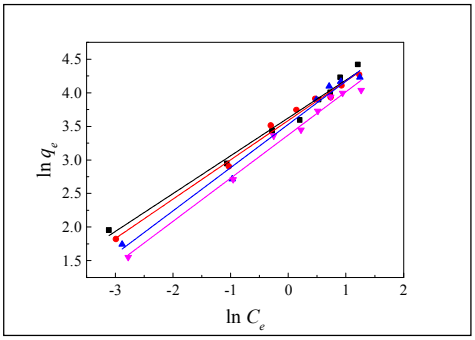

b

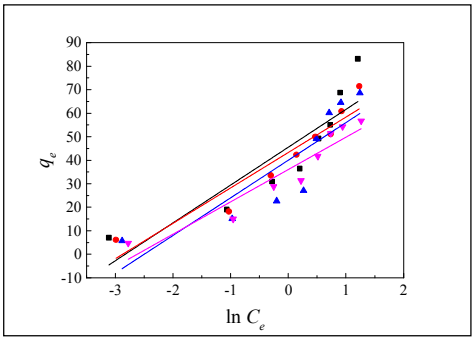

c

Fig. 11 Adsorption isotherm fits for the adsorption of p-nitrophenol by CD@Si, (a) Langmuir model, (b) Freundlich model, and (c) Tempkin model.
Conditions: ■283 K, ● 293 K, ▲303 K, ▼313 K. Initial pH of solution, 7.0. Solution volume of p-nitrophenol, 10.0 mL. Adsorbent CD@Si, 0.10 g. Shaking speed, 150 rpm. Contact time, 2.0 h.

Langmuir model and Tempkin model, which indicates that the distribution of adsorption sites on the surface of CD@Si are heterogeneous, and the stronger adsorption sites are occupied firstly. Both the correlation coefficients for Langmuir model and Tempkin model are lower than Freundlich model. The greater n value in Freundlich model in all the temperature involved means the adsorption process is favourable in a wide temperature range. Thus, in this work, the adsorption of p-nitrophenol onto CD@Si obeys the Freundlich model.

Table 3 The adsorption isotherm parameters for the adsorption of p-nitrophenol by CD@Si.

Model	Parameters	Parameter Value			
		283K	293K	303K	313K
Langmuir model	q_m (mg/g)	108.5	89.1	116.1	80.3
	K_L (L/g)	0.6144	0.8548	0.4048	0.7016
	R^2	0.7501	0.9330	0.4999	0.9277
Freundlich model	n	1.776	1.708	1.553	1.555
	K_F (mg/g)	37.53	36.13	34.10	29.13
	R^2	0.9845	0.9912	0.9833	0.9855
Tempkin model	k_1	16.09	15.06	16.00	13.74
	k_2	16.95	17.72	12.19	13.78
	R^2	0.7644	0.8913	0.7257	0.8840

3.6. Adsorption thermodynamics

In order to access the thermodynamics parameters, the adsorption isotherms of p-nitrophenol onto CD@Si was analyzed at 283K, 293K, and 303K in the initial concentration of 0.10 g/L, 0.50 g/L, and 4.00 g/L respectively. The plots of lnK_d versus 1/T were listed in **Fig. 12** and the thermodynamic parameters obtained from the slope and intercept following equation (10) were summarized in **Table 4**. It is obvious that the ΔG values (-7.474 kJ/mol ~ -11.91 kJ/mol) are negative at all the temperature and initial concentration studied, which means that the adsorption of p-nitrophenol onto CD@Si is a spontaneous process, and does not need any energy from external environment. We can also observe that the Gibbs free energy change (ΔG) increases as the increase in the temperature, which means that lower temperature favours the adsorption of p-nitrophenol onto CD@Si. The negative values of enthalpy change (ΔH) indicate that the adsorption of p-nitrophenol onto CD@Si is an exothermic process, which is consistent with the phenomenon that adsorption of p-nitrophenol onto CD@Si is more favourable at lower temperature. And the negative values of entropy change (ΔS) tell us that the randomness decreases when p-nitrophenol was adsorbed onto CD@Si. Thus, it is concluded from the adsorption thermodynamics study that the adsorption of p-nitrophenol onto CD@Si is a feasible, spontaneous and exothermic process, and this process is more favourable in lower temperature.

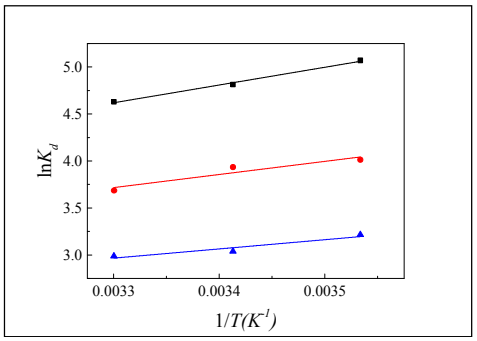

Fig. 12 Plots of lnK_d versus 1/T for the adsorption of p-nitrophenol by CD@Si. Conditions: ■0.10 g/L, ● 0.50 g/L, ▲ 4.00 g/L. Temperature, 283K, 293K, and 303K. Initial pH of solution, 7.0. Solution volume of p-nitrophenol, 10.0 mL. Adsorbent CD@Si, 0.10 g. Shaking speed, 150 rpm. Contact time, 2.0 h.

3.7. Reusability of CD@Si

Reusability is a very important requirement for adsorbent, which will reduce the material-cost significantly in practical application. The reusability of CD@Si in the adsorption of p-nitrophenol was illustrated in **Fig.13**. For the loss of adsorbent in each reusability experiment, the volume of p-nitrophenol aqueous solution added should be decreased proportionally in each run. From **Fig. 13**, it could be observed that as the reusability experiments were conducted in sequence for five runs, the equilibrium adsorption capacity decreased from 41.5 mg/g to 31.7 mg/g, an acceptable adsorption capacity, which is

View Article Online
DOI: 10.1039/C5RA15592D

about 76% of the initial adsorption capacity. The decrease in equilibrium adsorption capacity is mainly attributed to the incomplete desorption of p-nitrophenol from CD@Si. On the whole, considering the fast adsorption property, CD@Si is a promising adsorbent in practical application which can be reused at least five runs with acceptable adsorption capacity.

Table 4 The thermodynamic parameters for the adsorption of p-nitrophenol by CD@Si.

C_0 (g/L)	Temperature (K)	ΔH (kJ/mol)	ΔS (J/mol/K)	ΔG (kJ/mol)
	283			-11.91
0.10	293	-15.71	-13.44	-11.77
	303			-11.64
	283			-9.511
0.50	293	-11.60	-7.383	-9.437
	303			-9.363
	283			-7.519
4.00	293	-8.155	-2.249	-7.496
	303			-7.474

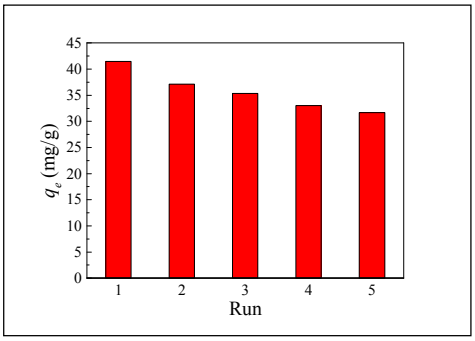

Fig. 13 Reusability of CD@Si in the adsorption of p-nitrophenol. Conditions: Initial concentration of p-nitrophenol, 2.00 g/L in 0.05 mol/L KH_2PO_4-K_2HPO_4 buffer solution. Solution volume of p-nitrophenol, 30.0 mL. Adsorbent CD@Si, 0.30 g. Shaking speed, 150 rpm. Temperature, 303 K. Contact time, 2.0 h.

3.8. Adsorption mechanism

Based on the systematical study on adsorption kinetics, adsorption isotherms, and adsorption thermodynamics above, the adsorption mechanism of p-nitrophenol onto CD@Si was speculated. In TGA spectrum of CD@Si (**Fig.5**), the amount of β-CD immobilized on the surface of hybrid silica is about 25% (m/m), so even if all the β-CD units form inclusion complexes with p-nitrophenol in the molar ratio of 1:1 as reported,[75-78] the maximum adsorption capacity of CD@Si to p-nitrophenol is about 30.6 mg/g. Considering the inclusion equilibrium between β-CD unit and p-nitrophenol, not all the β-CD unit could be occupied by p-nitrophenol, thus the maximum adsorption capacity in this work should be below 30.6 mg/g. But in fact, the maximum adsorption capacity is higher than 30.6 mg/g, especially in high initial concentration, 3.00 g/L and 4.00 g/L. Thus besides forming inclusion complexes, there is another interaction form between CD@Si and p-nitrophenol, which is hydrogen bond as reported in some similar literature.[54] The formation of inclusion complexes between β-CD unit and p-nitrophenol could be illustrated through the ^{1}H ROESY NMR study. Employing mono(6-ethylenediamine)-β-CD as the representative of β-CD unit on CD@Si, obvious correlation peaks between the H atoms located in the phenyl ring of p-nitrophenol and the H-3, H-5 in the cavity of the parent β-CD can be observed (**Fig. 14**), which is a strong evidence for the formation of inclusion complexes. The existence of hydrogen bond interaction is indicated through comparing the FT-IR spectra of CD@Si before and after the adsorption process as shown in **Fig. 15**. When p-nitrophenol was adsorbed onto CD@Si, the O-H stretching vibrations of β-CD unit on CD@Si shift from around 3388 cm^{-1} to around 3261 cm^{-1}, which is attributed to the formation of hydrogen bond between p-nitrophenol and the β-CD unit on CD@Si. And the appearance of peaks at 1592 cm^{-1} and 1496 cm^{-1} in the FT-IR spectrum of CD@Si after the adsorption process, is another powerful evidence to the adsorption of p-nitrophenol onto CD@Si, which belong to the stretching vibrations of C=C in phenyl ring. Thus, based on the analysis above, the adsorption mechanism of p-nitrophenol onto CD@Si can be summarized as shown in **Fig.16**. Inclusion complexes and hydrogen bond interaction are two origins of p-nitrophenol being adsorbed onto CD@Si.

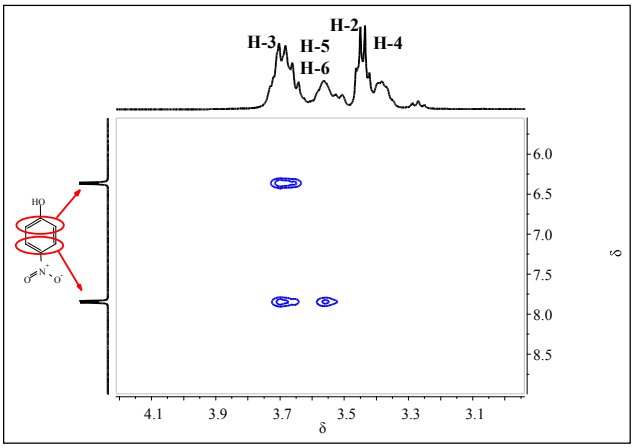

Fig. 14 Partial ^{1}H ROESY NMR spectrum of the inclusion complex between mono(6-ethylenediamine)-β-CD and p-nitrophenol.

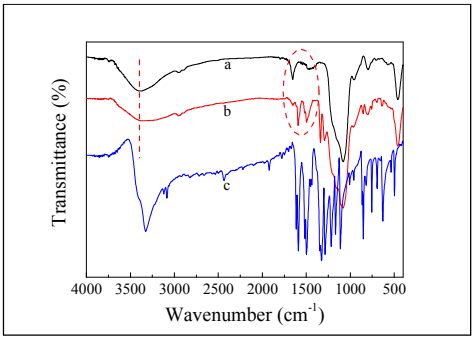

Fig. 15 FT-IR spectra of (a) CD@Si (before adsorption), (b) CD@Si (after adsorption), and (c) p-nitrophenol.

4. Conclusions

View Article Online
DOI: 10.1039/C5RA15592D

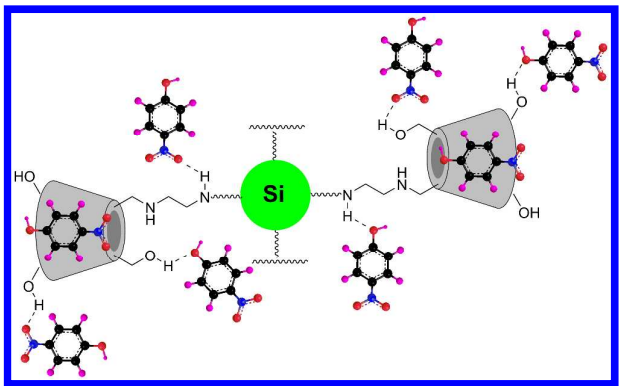

Fig. 16 Speculated adsorption mechanism of p-nitrophenol onto CD@Si.

In summary, reproducible β-CD has been immobilized onto the surface of hybrid silica successfully in this work, and the successful immobilization was confirmed through FT-IR, XPS, EDX, contact angle measurement, TGA, solid-state ^{13}C NMR, SEM, and XRD analyses. Applied in the adsorption of p-nitrophenol from aqueous phase, CD@Si exhibits satisfying fast-adsorption performance. The adsorption equilibrium can be reached in 15 s with acceptable equilibrium adsorption capacity of 69.6 mg/g in neutral condition (pH = 7.0), which is much faster than many reported adsorbents based on β-CD in the adsorption of p-nitrophenol or its analogues, which is mainly attributed to the maintenance of the hydrophobic cavity of β-CD and the distribution of β-CD unit on the surface of hybrid silica. The fast-adsorption performance demonstrates that CD@Si is a very suitable and promising adsorbent for fast adsorption in cases of emergency, when a large amount of p-nitrophenol was leaked to nature water. And the adsorption of p-nitrophenol onto CD@Si follows the pseudo-second-order adsorption model, obeys the Freundlich model, and is a feasible, spontaneous, and exothermic process, which is more favorable in lower temperature. Based on the adsorption mechanism study, it is concluded that, inclusion complex and hydrogen bond interaction are two origins of p-nitrophenol being adsorbed onto CD@Si. At last, from the perspective of economy, CD@Si can be recycled and reused at least five runs with acceptable adsorption capacity. In general, CD@Si is a very attractive candidate adsorbent in the fast adsorption of p-nitrophenol or its analogues from aqueous phase, especially in cases of emergency, and possesses promising application potential in the wastewater treatment without any additional environmental pollution in its application, which is a genuine environmental management strategy. And this work also provides a strategy to increase the adsorption rate of the adsorbent based on β-CD.

Acknowledgements

This work was supported by the National Natural Science Foundation of China (Grant No. 21306176, 21276006, 21476270), Scientific Research Launching Foundation of Zhejiang University of Technology (Grant No. G2817101103) and Zhejiang Provincial Natural Science Foundation (Grant No. LQ14B020002).

References

1 R. Arasteh, M. Masoumi, A. M. Rashidi, L. Moradi, V. Samimi and S. T. Mostafavi, *Appl. Surf . Sci.*, 2010, **256**, 4447.
2 W. Liu, X. Y. Jiang and X. Q. Chen, *Appl. Surf. Sci.*, 2014, **320**, 764.
3 A. E. Ofomaja and E. I. Unuabonah, *Carbohyd. Polym.*, 2011, **83**, 1192.
4 L. M. Cotoruelo, M. D. Marques, F. J. Diaz, J. Rodriguez-Mirasol, J. J. Rodriguez and T. Cordero, *Chem. Eng. J.*, 2012, **184**, 176.
5 B. Sarkar, Y. F. Xi, M. Megharaj, G. S. R. Krishnamurti and R. Naidu, *J. Colloid. Interf. Sci.*, 2010, **350**, 295.
6 S. Han, F. Zhao, J. Sun, B. Wang, R. Y. Wei and S. Q. Yan, *J. Magn. Magn. Mater.*, 2013, **341**, 133.
7 T. O. Isichei and F. E. Okieimen, *Environ. Pollut.*, 2014, **3**, 99.
8 Y. Y. Sun, J. B. Zhou, W. Q. Cai, R. S. Zhao and J. P. Yuan, *Appl. Surf. Sci.*, 2015, **345**, 897.
9 B. Sarkar, M. Megharaj, Y. F. Xi and R. Naidu, *Chem. Eng. J.*, 2012, **185**, 35.
10 B. J. Liu, F. Yang, Y. X. Zou and Y. Peng, *J. Chem. Eng. Data*, 2014, **59**, 1476.
11 O. E. A. A. Adam and A. H. Al-Dujaili, *J. Chem.*, 2013, http://dx.doi.org/10.1155/2013/694029.
12 Y. Park, G. A. Ayoko, R. Kurdi, E. Horvath, J. Kristof and R. L. Frost, *J. Colloid. Interf. Sci.*, 2013, **406**, 196.
13 F. Ahmad, W. M. A. W. Daud, M. A. Ahmad and R. Radzi, *Chem. Eng. J.*, 2011, **178**, 461.
14 G. H. Xue, M. L. Gao, Z. Gu, Z. X. Luo and Z. C. Hu, *Chem. Eng. J.*, 2013, **218**, 223.
15 J. Rivera-Utrilla, M. Sanchez-Polo, V. Gomez-Serrano, P. M. Alvarez, M. C. M. Alvim-Ferraz and J. M. Dias, *J. Hazard. Mater.*, 2011, **187**, 1.
16 M. H. Entezari and T. R. Bastami, *J. Hazard. Mater.*, 2006, **137**, 959.
17 T. R. Bastami and M. H. Entezari, *Chem. Eng. J.*, 2012, **210**, 510.
18 B. Zhang, F. Li, T. Wu, D. J. Sun and Y. J. Li, *Colloid. Surface. A*, 2015, **464**, 78.
19 O. Gimeno, M. Carbajo, F. J. Beltran and F. J. Rivas, *J. Hazard. Mater.*, 2005, **119**, 99.
20 M. Ksibi, A. Zemzemi and R. Boukchina, *J. Photoch. Photobio. A*, 2003, **159**, 61.
21 P. Canizares, J. Lobato, R. Paz, M. A. Rodrigo and C. Saez, *Water Res.*, 2005, **39**, 2687.
22 S. F. Shen, S. E. Kentish and G. W. Stevens, *Sep. Purif. Technol.*, 2012, **95**, 80.
23 P. Praveen and K. C. Loh, *J. Membrane Sci.*, 2013, **437**, 1.
24 S. W. Peretti, C. J. Tompkins, J. L. Goodall and A. S. Michaels, *J. Membrane Sci.*, 2002, **195**, 193.
25 Y. X. Yao, H. B. Li, J. Y. Liu, X. L. Tan, J. G. Yu and Z. G. Peng, *J. Nanomater.*, 2014, http://dx.doi.org/10.1155/2014/571745.
26 M. Erdem, E. Yuksel, T. Tay, Y. Cimen and H. Turk, *J. Colloid. Interf. Sci.*, 2009, **333**, 40.
27 B. Koubaissy, G. Joly, I. Batonneau-Gener and P. Magnoux, *Ind. Eng. Chem. Res.*, 2011, **50**, 5705.
28 J. H. Huang, C. Yan and K. L. Huang, *J. Colloid. Interf. Sci.*, 2009, **332**, 60.
29 J. Szejtli, *Chem. Rev.*, 1998, **98**, 1743.
30 R. Villalonga, R. Cao and A. Fragoso, *Chem. Rev.*, 2007, **107**, 3088.
31 F. Sallas and R. Darcy, *Eur. J. Org. Chem.*, 2008, 957.
32 M. A. Abdel-Naby, H. A. El-Refai and A. F. Abdel-Fattah, *J. Appl. Microbiol.*, 2011, **111**, 1129.

View Article Online
DOI: 10.1039/C5RA15592D

33 L. X. Zhang, H. Zhang, F. Gao, H. Y. Peng, Y. H. Ruan, Y. Z. Xu and W. G. Weng, *RSC Adv.*, 2015, **5**, 12007.
34 Y. J. Yao, X. W. Liu, T. Liu, J. Zhou, J. Zhu, G. Sun and D. N. He, *RSC Adv.*, 2015, **5**, 6305.
35 J. Q. Zhang, D. Wu, K. M. Jiang, D. Zhang, X. Zheng, C. P. Wan, H. Y. Zhu, X. G. Xie, Y. Jin and J. Lin, *Carbohyd. Res.*, 2015, **406**, 55.
36 N. Vilanova and C. Solans, *Food Chem.*, 2015, **175**, 529.
37 D. X. Wang, L. L. Liu, X. Y. Jiang, J. G. Yu, X. H. Chen and X. Q. Chen, *Appl. Surf. Sci.*, 2015, **329**, 197.
38 H. Q. Wu, J. H. Kong, X. Y. Yao, C. Y. Zhao, Y. L. Dong and X. H. Lu, *Chem. Eng. J.*, 2015, **270**, 101.
39 D. X. Wang, L. L. Liu, X. Y. Jiang, J. G. Yu and X. Q. Chen, *Colloid. Surface. A*, 2015, **466**, 166.
40 M. L. Wang, P. Liu, Y. Wang, D. M. Zhou, C. Ma, D. J. Zhang and J. H. Zhan, *J. Colloid. Interf. Sci.*, 2015, **447**, 1.
41 Y. B. Zhou, X. C. Gu, R. Z. Zhang and J. Lu, *Ind. Eng. Chem. Res.*, 2014, **53**, 887.
42 L. C. Zhou, X. G. Meng, J. W. Fu, Y. C. Yang, P. Yang and C. Mi, *Appl. Surf. Sci.*, 2014, **292**, 735.
43 L. D. Wilson, D. Y. Pratt and J. A. Kozinski, *J. Colloid. Interf. Sci.*, 2013, **393**, 271.
44 A. Celebioglu, S. Demirci and T. Uyar, *Appl. Surf. Sci.*, 2014, **305**, 581.
45 N. J. Wang, L. L. Zhou, J. Guo, Q. Q. Ye, J. M. Lin and J. Y. Yuan, *Appl. Surf. Sci.*, 2014, **305**, 267.
46 A. Z. M. Badruddoza, G. S. S. Hazel, K. Hidajat and M. S. Uddin, *Colloid. Surface. A*, 2010, **367**, 85.
47 Y. S. Ji, X. Y. Liu, M. Guan, C. D. Zha, H. Y. Huang, H. X. Zhang and C. M. Wang, *J. Sep. Sci.*, 2009, **32**, 2139.
48 L. B. de Carvalho, T. G. Carvalho, Z. M. Magriotis, T. D. Ramalho and L. D. A. Pinto, *J. Incl. Phenom. Macro.*, 2014, **78**, 77.
49 N. V. Roik and L. A. Belyakova, *J. Colloid. Interf. Sci.*, 2011, **362**, 172.
50 M. Chen, W. H. Ding, J. Wang and G. W. Diao, *Ind. Eng. Chem. Res.*, 2013, **52**, 2403.
51 X. D. Liu, L. Yan, W. Y. Yin, L. J. Zhou, G. Tian, J. X. Shi, Z. Y. Yang, D. B. Xiao, Z. J. Gu and Y. L. Zhao, *J. Mater. Chem. A*, 2014, **2**, 12296.
52 X. J. Hu, Y. G. Liu, H. Wang, G. M. Zeng, X. Hu, Y. M. Guo, T. T. Li, A. W. Chen, L. H. Jiang and F. Y. Guo, *Chem. Eng. Res. Des.*, 2015, **93**, 675.
53 L. P. Lukhele, R. W. M. Krause, B. B. Mamba and M. N. B. Momba, *Water Sa*, 2010, **36**, 433.
54 K. G. Chai and H. B. Ji, *Chem. Eng. J.*, 2012, **203**, 309.
55 A. G. Stamatis, D. Giasafaki, K. C. Christoforidis, Y. Deligiannakis and M. Louloudi, *J. Mol. Catal. A-Chem.*, 2010, **319**, 58.
56 G. Borja, A. Monge-Marcet, R. Pleixats, T. Parella, X. Cattoen and M. W. C. Man, *Eur. J. Org. Chem.*, 2012, 3625.
57 W. S. Guo, A. Monge-Marcet, X. Cattoen, A. Shafir and R. Pleixats, *React. Funct. Polym.*, 2013, **73**, 192.
58 H. M. Shen and H. B. Ji, *Tetrahedron Lett.*, 2012, **53**, 3541.
59 H. M. Shen and H. B. Ji, *Carbohyd. Res.*, 2012, **354**, 49.
60 H. M. Shen and H. B. Ji, *Tetrahedron*, 2013, **69**, 8360.
61 J. Li, C. L. Chen, Y. Zhao, J. Hu, D. D. Shao and X. K. Wang, *Chem. Eng. J.*, 2013, **229**, 296.
62 M. T. Sikder, Y. Mihara, M. S. Islam, T. Saito, S. Tanaka and M. Kurasaki, *Chem. Eng. J.*, 2014, **236**, 378.
63 J. Chen, R. J. Qu, Y. Zhang, C. M. Sun, C. H. Wang, C. N. Ji, P. Yin, H. Chen and Y. Z. Niu, *Chem. Eng. J.*, 2012, **209**, 235.
64 Q. Hu, D. W. Gao, H. Y. Pan, L. L. Hao and P. Wang, *RSC Adv.*, 2014, **4**, 40071.
65 L. L. Fan, C. N. Luo, M. Sun, H. M. Qiu and X. J. Li, *Colloid. Surface. B*, 2013, **103**, 601.
66 C. Sarmah, D. Sahu and P. Das, *Catal. Today*, 2012, **198**, 197.
67 X. H. Li, B. W. Zhao, K. Zhu and X. K. Hao, *Chinese J. Chem. Eng.*, 2011, **19**, 938.
68 L. L. Fan, M. Li, Z. Lv, M. Sun, C. N. Luo, F. G. Lu and H. M. Qiu, *Colloid. Surface. B*, 2012, **95**, 42.
69 J. M. Pan, X. H. Zou, X. Wang, W. Guan, C. X. Li, Y. S. Yan and X. Y. Wu, *Chem. Eng. J.*, 2011, **166**, 40.
70 W. C. E. Schofield, C. D. Bain and J. P. S. Badyal, *Chem. Mater.*, 2012, **24**, 1645.
71 H. Huang, Y. F. Fan, J. W. Wang, H. Q. Gao and S. Y. Tao, *Macromol. Res.*, 2013, **21**, 726.
72 A. M. Badruddoza, Z. B. Shawon, T. W. J. Daniel, K. Hidajat and M. S. Uddin, *Carbohyd. Polym.*, 2013, **91**, 322.
73 L. L. Li, L. L. Fan, H. M. Duan, X. J. Wang and C. N. Luo, *RSC Adv.*, 2014, **4**, 37114.
74 S. H. Lin and R. S. Juang, *J. Environ. Manage.*, 2009, **90**, 1336.
75 C. Yuan, Z. F. Lu, and Z. Y. Jin, *Food Chem.,* 2014, **152**,140.
76 F. Silva, A. Figueiras, E. Gallardo, C. Nerin and F. C. Domingues, *Food Chem.,* 2014, **145**, 115.
77 D. W. Wang, C. B. Ouyang, Q. Liu, H. L. Yuan and X. H. Liu, *Carbohyd. Polym.,* 2013, **93**, 753.
78 C. Manivannan, R. V. Solomon, P. Venuvanalingam and R. Renganathan, *Spectrochim. Acta A,* 2013, **103**, 18.

View Article Online
DOI: 10.1039/C5RA15592D

Graphical Abstract

Surface immobilization of *β*-cyclodextrin on hybrid silica and its fast-adsorption performance to *p*-nitrophenol from aqueous phase

Hai-Min Shen[a], Gong-Yuan Zhu[a], Wu-Bin Yu[a], Hong-Ke Wu[a], Hong-Bing Ji[b], Hong-Xin Shi[a], Yi-Fan Zheng[a*] and Yuan-Bin She[a*]

[a] *College of Chemical Engineering, Zhejiang University of Technology, Hangzhou 310014, China*

[b] *School of Chemistry and Chemical Engineering, Sun Yat-sen University, Guangzhou 510275, China*

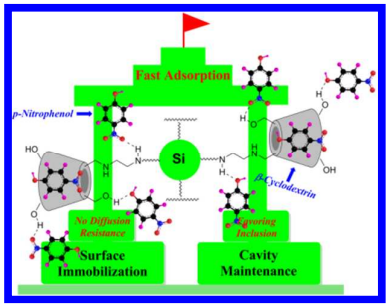

Fast-adsorption of *p*-nitrophenol was achieved through surface immobilization of *β*-cyclodextrin onto hybrid silica and maintenance of its hydrophobic cavity.

*Corresponding author. E-mail address: haimshen@zjut.edu.cn. Fax: (+86)571-8832-0533. Tel. : (+86)571-8832-0533.